Available online at www.sciencedirect.com

ScienceDirect

Procedia Manufacturing 44 (2020) 12–19

Procedia MANUFACTURING

www.elsevier.com/locate/procedia

1st International Conference on Optimization-Driven Architectural Design (OPTARCH 2019)

Shape Optimization of Assembled Single-Layer Grid Structure with Semi-Rigid Joints

Konstantinos Daniel Tsavdaridis [1]*, Ruoqiang Feng[2], and Fengcheng Liu[3],

[1]*Associate Professor of Structural Engineering, School of Civil Engineering, University of Leeds, Woodhouse Lane, LS2 9JT, Leeds, UK*
[2]*The Key Laboratory of Concrete and Prestressed Concrete Structures of Ministry of Education, Southeast University, Nanjing 211189, China*
[3]*PhD Candidate, School of Civil Engineering, University of Leeds, Woodhouse Lane, LS2 9JT, Leeds, UK*

Abstract: This paper takes the effect of the semi-rigid joints into account to optimise the assembled free-form single-layer grid structure. Based on the experimental results of the semi-rigid joints, finite element models of single-layer grid structure with semi-rigid joints are established, and virtual spring elements are used to simulate the joint stiffness. The optimisation process is completed with the parallel collaboration of ANSYS and MATLAB data. The research goal is to minimise the total strain energy. Genetic algorithm is used for the optimisation, and the nodal z-coordinates are chosen as variables. The effect of the semi-rigid joints on the shape optimisation is studied by changing the joint stiffness. With this method, the optimal shapes of assembled grid structure with different joint stiffness and improved buckling load are obtained.

Keywords: Free-form grid structures; Semi-rigid joints; Shape optimisation; Strain engergy

1. Main text

In the last two decades, the rise of computer-aided design and modelling techniques has enabled a new level of sophistication in the design of free-form grid structures [1]. A large amount of structures with attractive designs and eye-catching shapes have recently been erected. As it is known to all, the 21st century is an era of efficiency. Therefore, the assembled free-form grid shells are becoming a universal structural solution, enabling merger of

* Corresponding author. Tel.: +44(0)113 343 2299.
E-mail address: K.Tsavdaridis@leeds.ac.uk

10.1016/j.promfg.2020.02.199

structure and facade into a single layer skin, resulting in reduced labor costs and increased productivity. The assembled structure means that the connections of the rods are not connected through the welding joints but through the assembled joints. In practical applications, there are several types of assembly joints such as the German's metro-system [1], the Canadian Triodetic-system [3]-[4] and the American Temcor-system [5-6], as shown in Fig. 1. In recent years, some researchers have used the principle of topology optimisation to develop the assembly joints which as shown in Fig. 1 (d) **Error! Reference source not found.**.

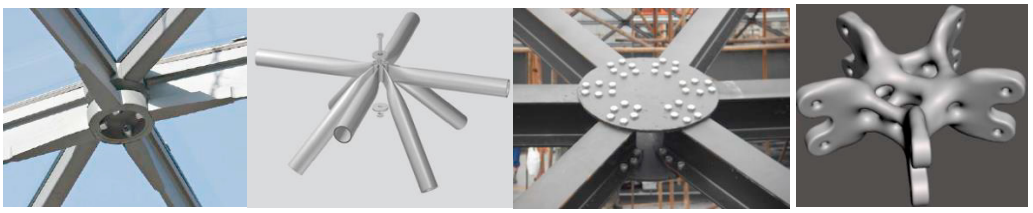

(a) metro-system (b) Triodetic -system (c) Temcor-system (d) Result of topology optimisation
Fig. 1 Some examples of assembly joints

With the development and wide use of assembly joints, the assembly single-layer free-form grid structure has become a hot spot in the research of large-span space structures. In addition, according to previous researches, most of the joints of the assembled grid structures are semi-rigid joints. It is generally known that the mechanical properties of connecting joints in assembled structures, such as strength and bending stiffness, have a great influence on the mechanical behaviour of the structure. Observations from earlier studies [8-10] confirmed that joint stiffness has a considerable effect on the load-displacement behavior of a structure. Various types of joints have been experimented for their respective mechanical performances, which have shown different effects on reticulated shells. L´opez et al. [11-12], Kato et al. [13] and Lightfoot [14]14] verified that the stiffness of the joints is an important factor that influences the behaviour of a single-layer latticed dome. It is worth noting that earlier studies on assembled free-form grid structures have mainly concentrated on the assemble connections and their influence on the stability of the structure; while to the authors' knowledge there no studies of shape optimisation of assembled single-layer grid structure considering the effects of semi-rigid joints.

With this background in mind, this paper takes the effect of the semi-rigid joints into account to optimise the assembled single layer grid structure. Firstly, based on experimental results of the semi-rigid joints, the spring elements are introduced to simulate the joint stiffness and then finite element models of assembled single-layer grid structure with semi-rigid joints are established. The effect of the semi-rigid joints on the shape optimisation is studied by changing the joint stiffness. Thereafter, the optimal shapes of assembled grid structure with different joint stiffness and improved buckling load are obtained. Finally, the mechanical properties of the optimised structure with rigid joints and the optimised assembly structure with semi-rigid joints are compared in detail.

2. Actual joint stiffness

In order to obtain the actual stiffness of the joint, the most direct way is to perform a joint prototype test. In this paper, the joint stiffness is obtained based on a prototype test called the 'central ring-sleeve joint test'. This kind of bolted joint is a self-developed joint that is suitable for free-formed single-layer grid structures. The mechanical properties of the joint have been thoroughly studied through both experiments and finite element analysis by the authors of this paper [15].

2.1 Construction Details of Ring-sleeve joint

The details of the construction of the Ring-Sleeve joint are shown as a sectional drawing in Fig. 2. The joint consists of a central ring, sleeves, tubes and high-strength bolts. There are identical bolt holes in the central ring, sleeve and

tube. The bolt holes of the central ring, sleeves and tubes are aligned to assemble the joint using the high-strength bolts.

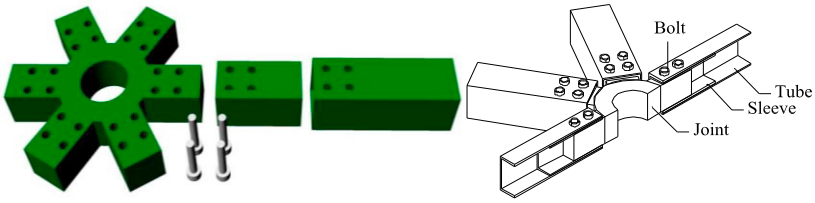

(a) Model of joint (b) Sectional drawing of joint

Fig. 2 Schematic diagram of joint

2.2 Mechanical property analysis of Ring-sleeve joints

In order to determine several mechanical indexes of the bolted joint, some prototype tests were carried out and the design parameters of the test joints are shown in Table 1 and Fig. 3. The loading device of joints test as shown Fig. 4.

Table 1. Geometrical parameters of the joint

Tube section	Joint No.	Joint			Bolt			Tube length	Sleeve		F/N
		R_1	R_2	L_1	Quantity	Diameter	Space	LL	L	Thickness	
100×100×4	1	50	95	135	4	16	80	715	180	4	0.02
	2	50	95	105	4	16	50	715	180	4	
	3	50	95	105	4	16	50	715	140	4	
	4	50	95	105	4	16	50	715	100	4	

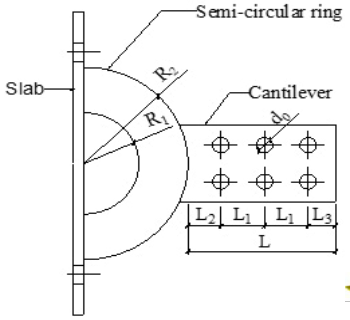

Fig. 3 Details of the semi-rigid joint

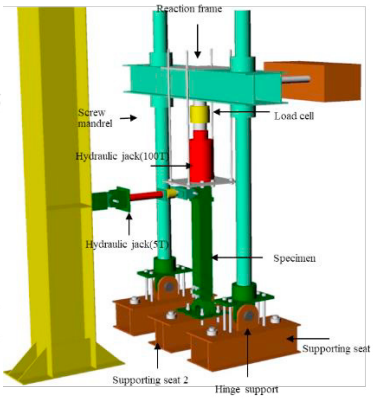

(a) Schematic presentation

(b) Loading diagram

Fig. 4 Test set up

The schematic diagram of loading was shown in Fig. 5. The ratio of the tube bending stress to the tube axial stress F-N can be confirmed as 0.02. For a rigid joint, the structure shown in the figure can be regarded as a cantilever beam. For the free end of the cantilever beam acts on the vertical downward concentrated load, the bending moment required for the unit angle of the cantilever beam is *3EI/LL*. Therefore, the rotational stiffness of the rod can be defined as *3EI/LL*, where the *E* represents the elastic modulus, *I* represents the moment of inertia and L*L* is the tube length. The rotational stiffness of the assembled joint is obtained by the prototype tests. Table 2 depicts the in-plane and out-plane rotational stiffness of four sets of central Ring-sleeve joints.

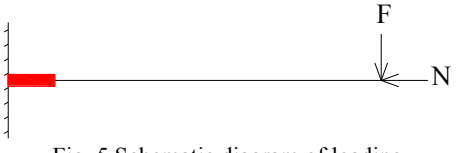

Fig. 5 Schematic diagram of loading

Table 2 The in-plane and out-plane rotational stiffness of the joints

Joint No.	Initial out-plane rotational stiffness (kN·m/rad)			Initial in-plane rotational stiffness (kN·m/rad)		
	Assembled joints	Rigid joints	Assembled joints / Rigid joints	Assembled joints	Rigid joints	Assembled joints / Rigid joints
1	1120	2042.77	0.55	180.77	2042.77	0.09
2	1030		0.50	166.24		0.08
3	922		0.45	148.81		0.07
4	781		0.38	126.05		0.06

It can be seen from Table 2 that the initial rotational stiffness of the Ring-Sleeve joint is smaller than the rotational stiffness of the rigid joint, and the average out-plane rotational stiffness of the Ring-Sleeve joint is about 47% of the rigid joint. For the out-plane initial rotational stiffness, the initial rotational stiffness of the Ring-Sleeve node is small, which is about 7.5% of the rigid joint. At the same time, according to the test results, the smaller the cross-section of the rod, the more rigid is the Ring-Sleeve joint.

3. Assembled single-layer grid structure with semi-rigid joints

3.1 Introducing the virtual spring elements

In the previous section, the actual rotational stiffness of the joint is obtained through the prototype tests. There are three ways to model small connections and simulate their behaviour. The first method is to build a solid model of joints and tubes. This yields the most accurate results but at the highest cost. Because both joints and rods need to be modelled by solid elements, the amount of calculation is very large, especially for the space grid structure which the number of joints and rods is extremely large. The second method is to build a multi-scale model. The multi-scale model simulates the change of stiffness of joint by reducing the cross-sectional area of the rod near the joint, which can accurately simulate the stiffness of the joint in the linear section, but its disadvantage is that the joint stiffness of the nonlinear section cannot be obtained. The most sophisticated method is to establish a bar-model that can consider the stiffness of the joint. This model considers the change of the stiffness of joint by introducing a nonlinear spring. In this paper, in order to study the influence of the stiffness of the assembled joint on the shape optimisation of single-layer grid structure, the latter method is used to consider the stiffness of the assembled joint.

Six virtual spring elements are used to simulate the freedom of six directions of joints, and the interaction between different rods and different degrees of freedom of joints is not considered. Therefore, the following two assumptions are proposed when using virtual springs to simulate the stiffness of joints:

(1) Ignore the mutual influence of the rod end stiffness between the two rods, and
(2) Ignore the interaction between the six springs of the same rod.

In the spatial grid structure, the axial stiffness of the joint is much larger than the bending stiffness, so it is believed that there is no axial tensile or compressive deformation between the joint and the rod in the assembled grid structure. That is to say the axial stiffness is defaulted to be infinite. According to relevant research, the maximum effect of torsional stiffness of joints on ultimate load of reticulated shells with different rise-span ratios is not more than 5%, and has no effect on the instability mode of the reticulated shell. Therefore, the effect of torsional stiffness of assembled joints on the mechanical properties of single-layer grid structures is not considered herein.
In addition, considering that the geometric size of the assembly joint is much smaller than the length of the rod, this paper ignores the influence of the size of the joint. The joint in this paper is replaced by a point in space, which is

called the central point. The coordinates of the central point are the same as those of the end point of the rod in the structure. In the numerical model of assembled free-formed single-layer grid structure, three nonlinear spring elements combin39 are used to simulate the rotational capacity of assembly joints in three directions, and three axial spring elements are used to simulate translational degrees of freedom in three directions.
The finite element model of Beam - Virtual Springs is shown in Fig. 6. Node 1 is the central node and node 2-7 are the discrete nodes.

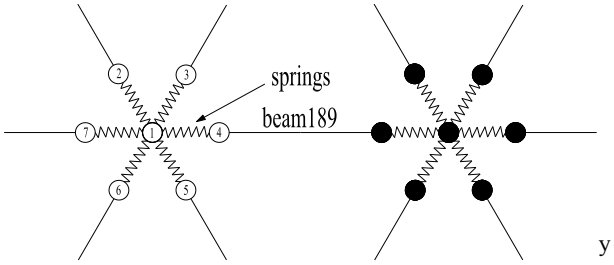

Fig. 6 Finite element model of beam-springs

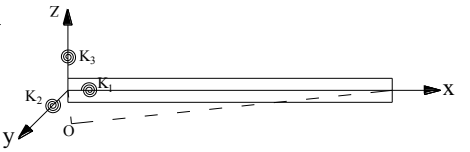

Fig. 7 Local coordinate system of spring element

Considering that the spatial grid structure has many spatial rods and joints, and each rod is located in different spatial positions, it is inconvenient to use virtual spring to simulate the joint stiffness. Therefore, in this paper, according to the orientation of each spatial rod, a local coordinate system is established with one end point of the rod as the origin, and the connecting direction of the two ends of the rod as the x-axis. Then a spring element is established in the local coordinate system, so that the spring element in each direction has a clear physical meaning. The local coordinate system of the spring element is shown in Fig.7.

3.2 Derivation of spring stiffness

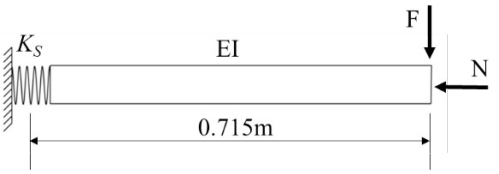

Fig. 8 Computational model with rotating spring

As shown in Fig. 8, it is the nodal calculation model with a rotating spring. Under the action of bending moment M, the deformation θ of the right end of the bar mainly includes the deformation θ_1 caused by the bending of the bar and the deformation θ_2 in the joint area. Assuming that the length of the bar is l, the elastic modulus is E, the cross-section inertia distance is I, the rotational stiffness of the bar is K_B, the spring at the end of the bar is a zero-length element, the rotational stiffness is K_S, and the rotational stiffness of the whole model is K_J.
According to structural mechanics:

Rotation angle of the rod: $$\theta_1 = \frac{M}{K_B}$$

Rotation angle of springs: $$\theta_2 = \frac{M}{K_S}$$

Total rotation of the joint: $$\theta = \frac{M}{K_J} = \theta_1 + \theta_2$$

Spring stiffness: $$K_S = \frac{K_J \times K_B}{K_B - K_J}$$

The rotational stiffness of the assembled joint model K_J is obtained by the test, and the final spring stiffness is shown in Fig. 9 and Fig. 10. Initially, the joint is in the elastic stage, and the spring stiffness remains unchanged. When the joint enters the plastic state, the spring stiffness gradually decreases. When the joint is damaged, the spring stiffness becomes 0, and the joint cannot continue to bear load.

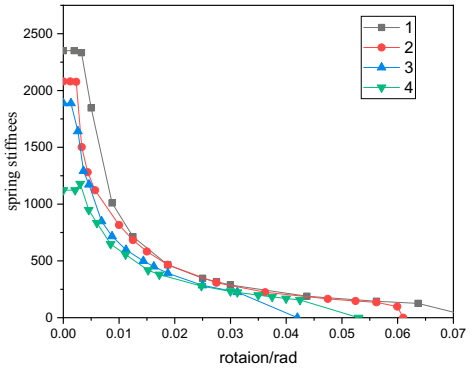

Fig. 9 Out-plane spring stiffness

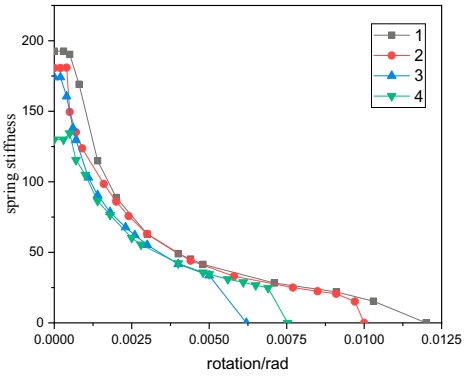

Fig. 10 In-plane spring stiffness

4. Shape optimisation of assembled single-layer grid structure with semi-rigid joints

4.1 Optimising parameters

Following established the finite element model of the assembled single-layer grid structure, the shape optimisation of the structure is completed in this section. As shown in Fig. 11, a triangular free-form single-layer grid structure with four edges articulated is examined, and the initial shape is defined as a free-form surface of 14m in span and 2.7m in height (the rise). The rod is the square steel tube with dimensions of 100mm×100mm×4mm made of Q345 steel, and the elastic modulus is $2.0\times10^5\,MPa$. The concentrated load is applied on each node as uniformly distributed load, including the rod weight, the finishing materials and the live load of 500 N/m^2.

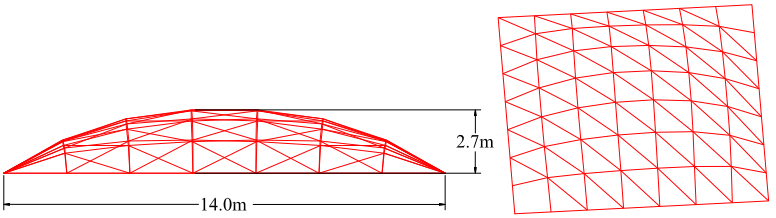

Fig. 11 A free-form single-layer grid structure

Objective function:

$$C(z)=\frac{1}{2}U^{T}KU \qquad \rightarrow Min$$

$$\text{Subject to} \begin{cases} \delta \le \dfrac{B}{400} \\ \sigma_{max} \le 345MPa \end{cases}$$

Where C is the total strain energy, K is the stiffness matrix, U is the nodal displacement vector, z is the nodal z-coordinate. B is the short span of the structure, δ is the maximum nodal displacement and σ_{max} is the maximum

stress of the tubes.

Design variables: For a free-formed single-layer spatial grid structure, the nodal coordinates are generally chosen as the design variables in the process of shape optimisation. Due to the change of the nodal vertical coordinate can change the structural form significantly, the z-direction coordinates of the internal nodes are set as design variables in this study. The range of the variables is [-1, 1], and 0 means the nodal original coordinates.

Optimisation algorithm: In the process of shape optimisation of free-form single-layer grid structure, constraints and objective functions are not only nonlinear but are generally implicit functions, so the choice of optimisation algorithm is very crucial. In this paper, the genetic algorithm is set as the optimisation algorithm. This kind of algorithm does not directly deal with variables, but achieves the optimisation purpose by encoding the variables. It does not need to calculate the function derivative information, and it has a good ability to solve complex optimisation problems.

4.2 Results

Table 3 Comparison of results

Model No.	Joint stiffness	Strain energy C/J	Buckling load P_u /N	Compare with rigid model
0	1.00	112.98	125960.0	100%
1	0.55	137.87	52320.4	41.50%
2	0.50	146.72	43437.4	34.49%
3	0.45	149.62	37506.0	29.77%
4	0.38	171.33	35156.0	27.91%

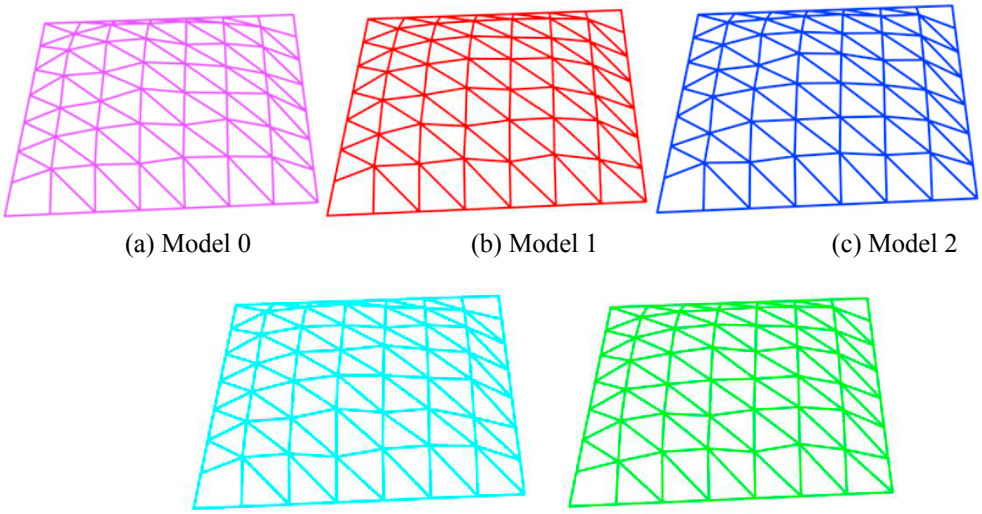

(a) Model 0 (b) Model 1 (c) Model 2

(d) Model 3 (e) Model 4

Fig. 12 Different shapes of the assembled grid structures with semi-rigid joints

Table 3 summarises the results of the shape optimisation considering the different joints stiffness; the contrast of shapes is shown in Fig. 12. It is worth noting that when the joint stiffness is 1.00, it represents a rigid joint, while the change of the stiffness of semi-rigid joint is represented by a proportion of the rigid joint. Model 0 is the optimisation result of the structure with rigid joint and model 1 - 4 are the results of the structures with semi-rigid joint. It can be seen from Table 3 and Fig. 12, when the joint stiffness of the free-form single-layer grid structure is changed, the optimised shape is different, and so is the structural buckling load capacity. Due to the sensitive to imperfections of the grid structures. The structural buckling load in table 3 is the result of considering the initial imperfection. In this paper, according to the consistent mode imperfection method, the least order mode of eigenvalue buckling mode is taken as the corresponding imperfection distribution mode. In specific, the smaller the

joint stiffness is, the smaller the structural buckling load capacity is. When the joint stiffness is 50% of the rigid joint, the buckling load capacity of the structure is only 34.49% of the rigid structure. The results shown that the difference of the stiffness of the joint will have an important impact on the final shape of the optimised structure. Therefore, the results obtained based on the rigid joint is not suitable for the assembled grid structures with semi-rigid joint. It is suggested to find the optimised final shape of the assembled free-form grid structure based on the semi-rigid joint directly.

5. Conclusions

It is generally known that the mechanical properties of connecting joints in assembled structures have significant influence on the mechanical behaviour of the structure. Therefore, the shape optimisation of the assembled free-form grid structure is herein considering the different joint stiffness. The virtual spring elements are used to simulate the joint stiffness, resulting to optimal shapes of assembled grid structures with different joint stiffness and improved buckling load capacity. The results also demonstrate that the optimised shape of the structure is very much dependent on the joint stiffness, this is to say, the smaller the joint stiffness is, the smaller the structural buckling load capacity is. Therefore, it is suggested as necessary to consider the influence of joint stiffness into consideration in the process of the shape optimisation of assembled free-form grid structure with semi-rigid joint.

Acknowledgements

This research was financially supported by the Colleges and Universities in Jiangsu Province Plans to Graduate Research and Innovation KYLX16_0254, and by the Fundamental Research Funds for the Central Universities, and by a Project Funded by the Priority Academic Program Development of the Jiangsu Higher Education Institutions.

References

[1] Rippmann M. Funicular Shell Design: Geometric approaches to form finding and fabrication of discrete funicular structures. ETH Zurich, (2016).
[2] MERO GmbH, P.Kraus. Patent 42 24 663 C2, German Patent Office, Munich, Germany, (1994).
[3] Lopez E. A. and Troup K. Aluminum lattice structures: Developments and innovations ion clear span roof solutions. International Symposium on Conceptual Design of Structures. (1996).
[4] Sugizaki K. and Kohmura S. Experimental study on buckling behavior of a triodetic aluminum space frame. Proceedings of the IASS-ASCE International Symposium, (1994), 478-487.
[5] Guo X, Xiong Z, Luo Y. The design method and detailed requirements of bearing capacity of aluminum alloy gusset joint. (2015).
[6] Guo X, Xiong Z, Luo Y, L Qiu, J Liu. Experimental investigation on the semi-rigid behavior of aluminium alloy gusset joints. Thin-walled structures, (2015), 87:30-40.
[7] Abdelwahab, M. and Tsavdaridis, K.D. Optimised 3D-Printed Metallic Node-Connections for Reticulated Structures. The 9th International Conference on Steel and Aluminium Structures. 3-5 July (2019), Bradford, UK.
[8] See, T. Large displacement elastic buckling of space structures. Doctoral Thesis, University of Cambridge, (1983).9.
[9] Fathelbab F.A. The effect of joints on the stability of shallow single layer lattice domes. Doctoral Thesis, University of Cambridge, (1987). 9.
[10] Fathelbab F.A. and McConnel R.E. Approximate tangent stiffness matrix includes the effects of joint properties for space frame member. Proceedings of the IASS congress, Madrid (1989), 5.
[11] L´opez, A., Puente, I. and Serna Miguel, A. Direct evaluation of the buckling loads of semi-rigidly jointed single-layer latticed domes under symmetric loading. Engineering Structures. (2007a). 29(1), 101–109.
[12] L´opez, A., Puente, I. and Serna Miguel, A. Numerical model and experimental tests on single-layer latticed domes with semi-rigid joints. Computers and Structures. (2007b). 85(7–8), 360–374.
[13] Kato, S., Mutoh, I. and Shomura, M. "Collapse of semi-rigidly jointed reticulated domes with initial geometric imperfections." J. Constr. Steel Res., (1998). 48(2–3), 145–168.
[14] Lightfoot, E. and Le Messurier, A. Instability of space frames having elastically connected and offset members. In Second International Conference on Space Structures, University of Surrey, Guildford, England. (1975, September).
[15] Feng R., Liu F., Yan G, X Chang. Mechanical behavior of Ring-sleeve joints of single-layer reticulated shells. Journal of Constructional Steel Research, (2017), 128: 601-610.